Rapid Communications

Evolution of field-induced metastable phases in the Shastry-Sutherland lattice magnet TmB$_4$

D. Lançon [1,2,3,*], V. Scagnoli,[2,3] U. Staub [4], O. A. Petrenko,[5] M. Ciomaga Hatnean [5], E. Canevet,[1] R. Sibille,[1] S. Francoual [6], J. R. L. Mardegan,[4] K. Beauvois,[7] G. Balakrishnan,[5] L. J. Heyderman [2,3], Ch. Rüegg [8,9] and T. Fennell [1,†]

[1]*Laboratory for Neutron Scattering and Imaging, Paul Scherrer Institute, 5232 Villigen PSI, Switzerland*
[2]*Laboratory for Mesoscopic Systems, Department of Materials, ETH Zurich, 8093 Zurich, Switzerland*
[3]*Laboratory for Multiscale Materials Experiments, Paul Scherrer Institute, 5232 Villigen PSI, Switzerland*
[4]*Swiss Light Source, Paul Scherrer Institut, 5232 Villigen PSI, Switzerland*
[5]*Department of Physics, University of Warwick, Coventry CV4 7AL, United Kingdom*
[6]*Deutsches Elektronen-Synchrotron (DESY), Hamburg 22607, Germany*
[7]*Institut Laue Langevin, CS 20156, Cedex 9, 38042 Grenoble, France*
[8]*Neutrons and Muons Research Division, Paul Scherrer Institute, 5232 Villigen PSI, Switzerland*
[9]*Department of Quantum Matter Physics, University of Geneva, 1211 Geneva, Switzerland*

The appearance of a plateau in the magnetization of a quantum spin system subject to continuously varying magnetic field invites the identification of a topological quantization. Indeed, the magnetization plateaus at 1/8 and 1/2 of saturation in TmB$_4$ have been suggested to be intrinsic, resulting from such a topological quantization, or, alternatively, to be metastable phases. By means of neutron- and x-ray-scattering experiments and magnetization measurements, we show that the 1/8 plateau is metastable, arising because the spin dynamics are frozen below $T \approx 4.5$ K. Our experiments show that in this part of the phase diagram of TmB$_4$, many long-ranged orders with different propagation vectors may appear and coexist, particularly as the applied field drives the system from one plateau to another. The magnetic structures accommodating a magnetization of $\approx 1/8$ seem to be particularly favorable, but still only appear if the system has sufficient dynamics to reorganize into a superstructure as it is driven toward the expected plateau. This work demonstrates that TmB$_4$ represents a model material for the study of slow dynamics, in and out of equilibrium.

Ising spin systems can have remarkably slow dynamics, because of the improbability of flipping spins at low temperature [1]. This means that the dynamics are frozen on reasonable experimental timescales, allowing the study of magnetic field or temperature quenches, and out-of-equilibrium phenomena in well-defined lattice models [2]. For example, in spin ice [3], individual spin flips are point defects [4] in a correlated but disordered background [5,6], and both reaction-diffusion phenomena and avalanche responses can be observed [7–9]. In other Ising spin systems with competing interactions, generally known as ANNNI (anisotropic next-nearest-neighbor interaction) models, a succession of phase transitions accompanied by a devil's staircase of propagation vectors [10–12] points to a rather flat energy landscape with many nearby ordered states formed by changing the population and organization of elements such as stripes or blocks of flipped spins. In materials such as CeSb [13] or Ho [14], successive states of the staircase are accessible via equilibrium phase transitions. However, the question of how such a system evolves when the staircase of states occurs at temperatures below which the spins fall out of equilibrium remains to be explored.

In TmB$_4$, the Tm^{3+} ($J = 6$) ions have a pseudodoublet ground state with dominant $m_j = \pm 6$ components and large ($6.6\mu_B$) Ising-like magnetic moments, located on a Shastry-Sutherland lattice (SSL) [15]. When a magnetic field H is applied along the tetragonal fourfold c axis (space group $P4/mbm$) at $T \approx 2$ K, fractional magnetization (M) plateaus emerge at $M \sim 1/8M_{\text{sat}}$ ($1.4 \lesssim \mu_0 H \lesssim 1.8$ T) and $M \approx 1/2M_{\text{sat}}$ ($1.8 \lesssim \mu_0 H \lesssim 3.5$ T) of the saturation magnetization (M_{sat}) [16,17], as in the phase diagram shown in Fig. 1 [17]. The 1/2 plateau can be explained by calculations of the ground state of frustrated Ising models on a SSL [18–28] but the 1/8 plateau is more difficult to rationalize. It appears in some models, but interpretations in terms of complex structures at domain walls [17] or incommensurate modulated magnetic order [29,30] have also been proposed. A connection between the magnetization plateaus of TmB$_4$ and the quantum Hall effect was made via a theory mapping a spin system to a two-dimensional electron gas [31–33]. Although this theory may be relevant to the well-known $S = 1/2$ Shastry-Sutherland lattice compound SrCu$_2$(BO$_3$)$_2$ [34,35], hysteresis effects [17], temperature-dependent values of the magnetization in the plateau [29], and thermodynamic measurements [36] show that the 1/8 plateau in TmB$_4$ is metastable, so such a theory is probably not relevant to TmB$_4$. Similar phase diagrams with fractional plateaus and multiple ordered phases are observed for other members of the series of RB$_4$, with R = Nd, Tb, Dy, Ho, Er [16,37–42].

In this work, we have made detailed investigations of TmB$_4$ using neutron- and x-ray-scattering and magnetization

*diane.lancon@psi.ch
†tom.fennell@psi.ch
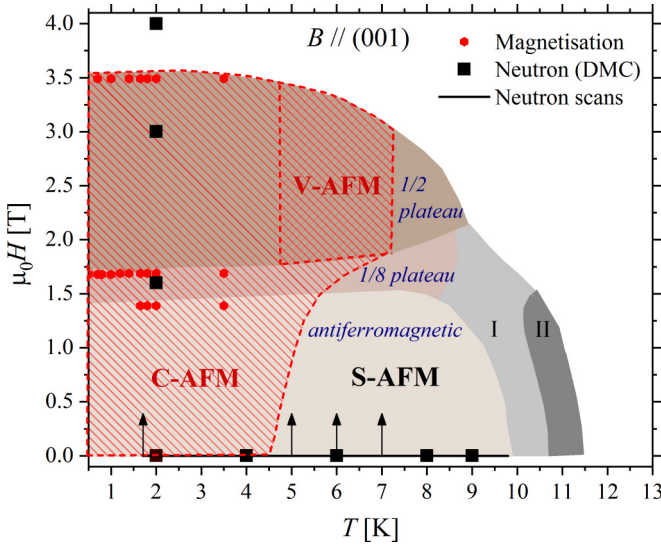
FIG. 1. The phase diagram of TmB$_4$ based on magnetization measurements [17] is shown by shaded regions and labeled in italics; our phase diagram includes the hatching and labels in bold font. The transition fields from upward field sweeps in our low-temperature magnetization measurements (see Fig. 2) are shown as red circles, squares indicate the positions of neutron diffraction maps measured in this work, while the black line and arrows correspond to neutron $\vec{Q}$ scans. Within the red dashed lines, the system may be in different metastable states, typically transitioning amongst them at the boundaries of the underlying magnetization phase diagram. C-AFM magnetic order is a coexistence of AFM Bragg peaks, incommensurate Bragg peaks, and strong $\vec{Q}$-dependent diffuse scattering. The S-AFM region corresponds to a simpler AFM order with weak diffuse scattering. The V-AFM region corresponds to a phase where both AFM Bragg peaks and various incommensurate propagation vectors were observed. I and II are modulated phases [17] not discussed in this Rapid Communication.

measurements. At low temperature, we find a frozen regime in which many history-dependent states appear as the system is driven from one plateau to another. These states are characterized by long-ranged orders with different propagation vectors, which may coexist with one another and may also coexist with short-ranged correlations. We suggest that the temperature, field, and history dependencies of the 1/8 plateau are a consequence of different degrees of self-organization into superstructures, depending if the system passes from one plateau to another in equilibrium or by quenching.

Tm^{11}B$_4$ single crystals were grown by the floating zone technique detailed in [43,44], using ^{11}B to minimize neutron absorption. Single-crystal neutron-scattering experiments in an applied field were carried out on the following instruments: the cold neutron diffractometer DMC, the single-crystal thermal neutron diffractometer ZEBRA, the thermal neutron triple-axis spectrometer EIGER at the Paul Scherrer Institute, and the thermal neutron diffractometer D23 at the Institut Laue-Langevin. Resonant x-ray-scattering experiments were also carried out in the soft x-ray range at RESOXS [45] at the SIM beamline [46] of the Swiss Light Source, and in the hard x-ray range at P09 at DESY, at the Tm M_5 and L_3 edges, respectively. In the scattering experiments, we
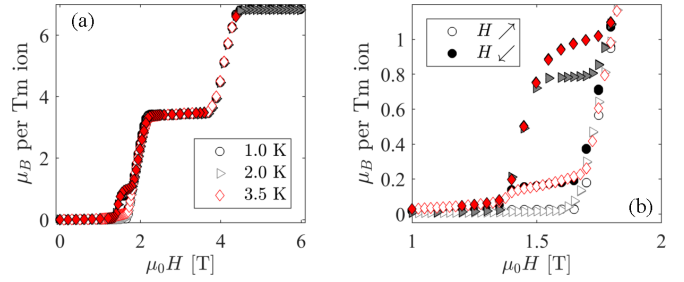
FIG. 2. Magnetization measurements on TmB$_4$ show the two plateaus (a), but inspection of the 1/8 plateau (b) shows that the value of the magnetization within the plateau is strongly temperature dependent, and that for $T \lesssim 2$ K the plateau completely disappears from the upward sweep.

either mapped regions of the $(h, k, 0)$ plane, or made scans through particular scattering features as a function of the wave vector ($\vec{Q}$). Magnetization measurements were made using a superconducting quantum interference device magnetometer with a ^{3}He insert. Results obtained in the history-dependent regime are reproduced only by using a specific protocol that ensures that different observations at a given point of the phase diagram are comparable. We used a field protocol (FP) described originally by Sunku *et al.* [17] to minimize hysteresis effects. The FP consists of zero-field cooling to a given temperature, followed by a field ramp up to 5 T and then back down to 0 T.

Magnetization measurements show that the 1/2 plateau is rather stable, always having $M \approx 1/2M_{\text{sat}}$ (though it is not perfectly flat) and appearing for $T < 10$ K. The 1/8 plateau typically appears when the FP is performed at $T \sim 2$ K, where it is most pronounced on the downward sweep. Our measurements, which extend to lower temperatures than those described in Refs. [17,36,39,47], show that in the downward sweep at $T = 3.5$ K, $M \approx 1/7M_{\text{sat}}$, for $T \approx 2$ K, $M \approx 1/8M_{\text{sat}}$, and at progressively lower temperatures the plateau further diminishes [43]. For the upward sweep, the plateau is entirely absent for $T < 2$ K, as shown in Fig. 2.

To investigate the phase diagram further, we performed neutron- and x-ray-scattering experiments. When cooled in zero field, TmB$_4$ first passes through two long-range-ordered equilibrium phases ($T_{N1} = 11.7$ K; $T_{N2} = 10.8$ K) before entering the Néel ordered antiferromagnetic (AFM) phase below $T_N = 10$ K (S-AFM in Fig. 1). This phase has propagation vector $\vec{k} = (1, 0, 0)$, resulting in magnetic Bragg peaks at $(1,0,0)$ and $(1,1,0)$. As this phase is further cooled to 2 K, neutron-scattering experiments show the development of diffuse scattering, which extends out of the magnetic Bragg peaks along the $(h, 0, 0)$ and $(0, k, 0)$ directions [as shown in Fig. 3(a)]. These streaks of diffuse scattering indicate that the ordered spin system fragments into many small square domains: The cross shape originates from the convolution of the Bragg scattering with a two-dimensional box function [48]. X-ray-scattering experiments show that the correlation length is much longer parallel to the c axis [43], implying a three-dimensional system as for HoB$_4$ [49]. After the FP, the system returns to a different state at 2 K and zero field, characterized by Bragg peaks with propagation vector $\vec{k} = (1, 0, 0)$
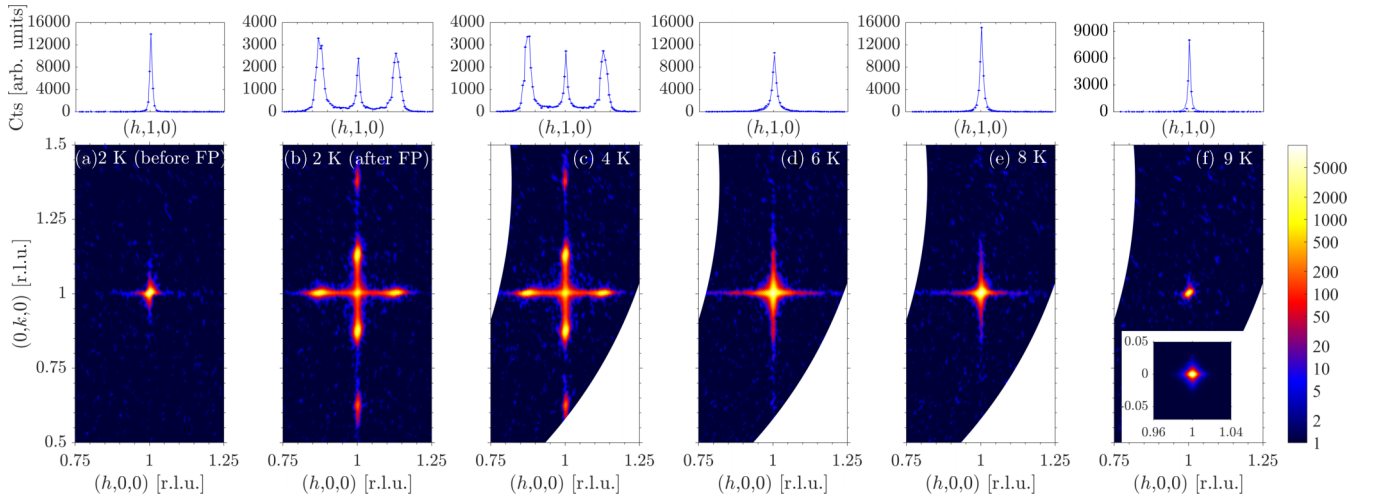
FIG. 3. Neutron-diffraction pattern at 2 K and zero field prior to the FP, showing a magnetic Bragg peak at (1,1,0), as well as weak diffuse scattering (a). After the FP the magnetic Bragg peak (1,1,0) coexists with magnetic Bragg peaks with propagation vector $\vec{k} = (1 \pm \delta, 0, 0)$ with $\delta = 1/8$ and 3δ (b). With increasing temperature [(c), (d), (e)], the peaks at $\vec{k} = (1 \pm \delta, 0, 0)$ disappear, leaving the magnetic Bragg peak at (1,1,0) and pronounced diffuse scattering. By 9 K (e), the Bragg peak appears resolution limited for neutron diffraction, but a measurement of the (1,0,0) AFM Bragg peak by resonant x-ray scattering (Tm M_5 edge) with a similar temperature and no field history [43] shows that the Bragg peaks still have a crosslike intensity distribution (inset). Data from DMC; the color scale represents the neutron intensity in arbitrary units.

and $\vec{k} = (1 \pm \delta, 0, 0)$ (plus equivalent $\vec{k}$ domains and $3\vec{\delta}$ harmonics) with $\delta \approx 1/8$, as well as a cross of diffuse scattering [Fig. 3(b)]. An average domain size of 590 ± 30 Å is estimated from the width of the arms of the diffuse cross, though the co-existence of two long-range orders and diffuse scattering suggests that there are many domain sizes in the system.

A mixture of domains of different antiferromagnetic structures is consistent with the zero net magnetization measured at low temperature and zero field (Fig. 2 and Refs. [39,47]). Its existence shows that the dynamics in the sample have become so slow that the system remains frozen in a metastable mixed state. This is further evidenced by using different speeds in the field ramp down from the 1/2 plateau, which produces different intensity distributions [43]. Slower ramping favors the $\vec{k} = (1, 0, 0)$ peaks (Fig. 4), suggesting that this is the equilibrium state at zero field.

On raising the temperature (after the FP, in zero field), the remnant $\vec{k} = (1 + \delta, 0, 0)$ phase melts at $T \approx 4.5$ K and the system relaxes back to the Néel structure [Figs. 3(b)–3(f) and [43]]. This process is reflected by the diminishing intensity of the incommensurate peaks until they vanish into the diffuse cross [Figs. 3(b)–3(d)]. As the incommensurate peaks disappear, their propagation vector softens toward $\vec{k} = (1, 0, 0)$ [43], suggesting that the superstructure reorganizes so that its periodicity lengthens until it collapses, leaving small $\vec{k} = (1, 0, 0)$ domains. By $T \sim 9$ K, the $\vec{k} = (1, 0, 0)$ Bragg peaks are resolution limited for neutron diffraction [Fig. 3(f)], though the cross can still be detected in x-ray-scattering experiments with finer wave-vector resolution [inset of Fig. 3(f)].

In neutron- and x-ray-scattering experiments, for all FP sweeps we have performed ($T \leqslant 7$ K), we observe well-defined plateaus with essentially field-independent intensities between sharp boundaries, as in Fig. 4. However, states with different propagation vectors [i.e., variable δ in

$\vec{k} = (1 + \delta, 0, 0)$] appear at different temperatures and at the transitions between the plateaus [43]. The propagation vector observed within a plateau at a given temperature is frozen, but may differ between the upward and downward field sweep; in the boundary region between plateaus the propagation vector may change continuously or discontinuously. Mixed states observed at the end of the FP have propagation vectors that depend on the temperature at which the FP was performed [43].
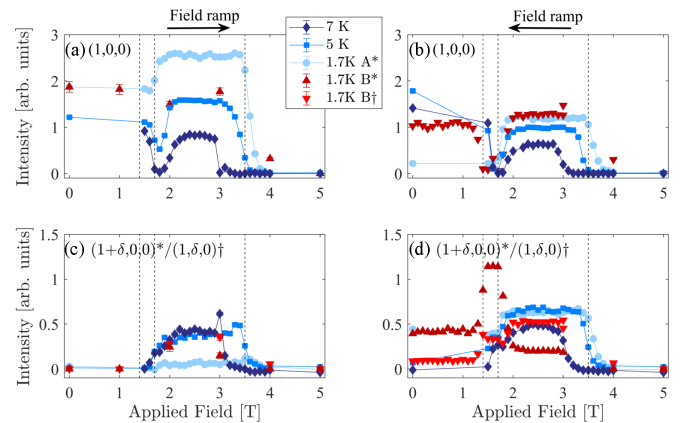
FIG. 4. Field evolution of the integrated intensity of Bragg peaks $\vec{Q} = (1, 0, 0)$ [panels (a) and (b)], $\vec{Q} = (1 + \delta, 0, 0)$, and $\vec{Q} = (1, \delta, 0)$ [panels (c) and (d)] with temperature. Note that δ is different (or even multiple) at different points in the phase space, but all superstructure intensity has been integrated. Two loops were done at 1.7 K with faster and slower ramping speeds, measurements A and B, respectively. The latter loop shows that the behavior of the $\vec{k} = (1 + \delta, 0, 0)$ ($\star$) and $\vec{k} = (1, \delta, 0)$ (†) domains may be different. Plateau boundaries from the phase diagram are indicated by dotted lines. Data from EIGER.

In Fig. 4 we compare the integrated intensity of the $\vec{k} = (1, 0, 0)$ and $\vec{k} = (1 + \delta, 0, 0)$ during field ramps. It should be noted that the incommensurate peak may appear at different values of δ at different points of the field/temperature history, but we use the integrated intensity to compare the proportion of the system that is ordered in simple or super structures. During upward field ramps for $T > 4.5$ K, the $\vec{k} = (1, 0, 0)$ peaks established in zero field pass through a distinctive minimum in intensity in the field range of the 1/8 plateau. Then they are reestablished in the 1/2 plateau and disappear in the high-field state. The $\vec{k} = (1 + \delta, 0, 0)$ peaks appear as the $\vec{k} = (1, 0, 0)$ peaks pass through the minimum, and then the $\vec{k} = (1 + \delta, 0, 0)$ peaks remain in the 1/2 plateau before disappearing in the high-field state. The downward sweep is similar, but different relative intensities and values of δ may occur in and between the plateaus. For $T < 4.5$ K, the simultaneous decrease of $\vec{k} = (1, 0, 0)$ and appearance of $\vec{k} = (1 + \delta, 0, 0)$ that is seen on the downward sweep, does not typically occur on the upward sweep. In the minimum of intensity for the $\vec{k} = (1, 0, 0)$ peaks on the downward sweep that signifies the $\approx 1/8$ plateau, different arms of the star of $\vec{k} = (1 + \delta, 0, 0)$ may have a different evolution: Either a weak evolution between the 1/2 plateau and zero magnetization state, or a strong maximum appears in Fig. 4. The intensities at the lower edge of the plateau are then frozen in without further change, forming the mixed state.

From these various observations, we can identify the consequences of the Ising-like spin anisotropy and competing interactions that determine the behavior of TmB$_4$. The competing interactions mean that there are many nearby low-energy states, and the strong anisotropy means that the spin dynamics become so slow that they freeze. Apparently this freezing occurs at a temperature lying within or just above the energy bandwidth of these states. Above the freezing temperature, the dynamics are active and the system explores all possible ground states induced by the applied field [43]. The Shastry-Sutherland lattice in TmB$_4$ has a four-atom basis with a $(+ - + -)$ configuration of Ising moments in the $\vec{k} = (1, 0, 0)$ Néel structure at zero field (see Fig. 3 in [30]). In the 1/8 plateau about one spin in four unit cells must be flipped (depending on the exact value of the magnetization) and in the 1/2 plateau, one spin per unit cell must be flipped to obtain the required magnetization. Although the 1/2 plateau can be accounted for with a 3-up-1-down structure in every unit cell, which would be broadly in agreement with the relative intensity changes of the $\vec{k} = (1, 0, 0)$ peaks, it appears that a proportion of these spin flips form a more complicated superstructure, giving rise to the $\vec{k} = (1 + \delta, 0, 0)$ peaks. As the field further changes the population of spin flips at transitions between plateaus, the system responds by rearranging them into superstructures (or soliton lattices) with the most energy-efficient periodicity. As a consequence we observe continuously or discretely varying propagation vectors, reminiscent of the floating phase and devil's staircase of some ANNNI models, respectively [12]. The proliferation of domain walls as the plateau states are converted back to the Néel state, evidenced by the cross of diffuse scattering, suggests that extended structures of spin flips have a low energy in the types of structure that exist in this parameter space.

The superstructure associated with the 1/8 plateau appears to be particularly favored: When the dynamics are active, it can organize on upward or downward field sweeps, almost completely suppressing any other structures. Below the freezing temperature, the field creates dynamics only when it brings the system to a point where two structures are degenerate, and, since the ramp rate in all our experiments (T min^{-1}) is rapid compared to any decay of the frozen structures (at least hours), the transitions correspond to quenches. Only small degrees of self-organization can occur as the system is driven from one plateau to another, requiring avalanchelike spin reconfigurations, hence the superstructures are less pronounced and sudden changes of intensity without evolution of the propagation vector are seen between plateaus.

Considerable efforts have been dedicated to models of TmB$_4$ with competing further neighbor (i.e. Ruderman-Kittel-Kasuya-Yoshida) interactions, which can be parametrized to produce long-range ordered phases in both 1/2 and 1/8 plateaus [18–28]. Experiments are usually interpreted in terms of simple structures implied by idealized values of the plateau magnetization (e.g., [31,36]). However, we show that history-dependent values of M occur within the $\sim 1/8$ plateau, and that different structures with different periodicities occur in and between the plateaus, and may coexist in history-dependent proportions (Figs. 2, 3 and 4, [43]; see also Ref. [31]). At low temperature the state of TmB$_4$ is therefore not well characterized as a long-range ordered phase with a unique value of the magnetization.

Our experiments suggest that the theoretical question of most importance in understanding TmB$_4$ is how a spin system negotiates the complex energy landscape of such models with limited dynamics. Some efforts in this direction have already identified firstly, the possibility of metastable coexisting states in ANNNI models [50], and, secondly, in a model of TmB$_4$ [23], history-dependent plateau magnetization and interconversion of phases by proliferation of domain walls in a manner qualitatively similar to that described above. A detailed description of the periodicity of the structures observed in TmB$_4$, the reasons for the particular stabilization of those with $\delta \approx 1/8$, and the mechanism of their interconversion has not been achieved. Undoubtedly this would be assisted by experimental efforts to trap the system in fully characterized states whose structure can be fully determined.

The puzzling low-temperature magnetic behavior of TmB$_4$ appears to result from a combination of frustration and slow dynamics. There are many ordered structures, but those with $\vec{k} = (1, 0, 0)$ and $\vec{k} = (1 + \delta, 0, 0)$ with $\delta \approx 1/8$ seem to be favored, leading to the regular observation of the 1/8 magnetization plateau when dynamics are sufficient for the system to reorganize itself in the region of phase space where this structure is stable.

The data that support this study are available via the Zenodo repository [51].

---

[1] J. Villain, Physica B+C **79**, 1 (1975).

[2] R. Stinchcombe, Adv. Phys. **50**, 431 (2001).

[3] M. Harris, S. Bramwell, D. McMorrow, T. Zeiske, and K. Godfrey, Phys. Rev. Lett. **79**, 2554 (1997).

[4] C. Castelnovo, R. Moessner, and S. L. Sondhi, Nature (London) **451**, 42 (2008).

[5] D. J. P. Morris, D. A. Tennant, S. A. Grigera, B. Klemke, C. Castelnovo, R. Moessner, C. Czternasty, M. Meissner, K. C. Rule, J.-U. Hoffmann, K. Kiefer, S. Gerischer, D. Slobinsky, and R. S. Perry, Science **326**, 411 (2009).

[6] T. Fennell, P. P. Deen, A. R. Wildes, K. Schmalzl, D. Prabhakaran, A. T. Boothroyd, R. J. Aldus, D. F. Mcmorrow, and S. T. Bramwell, Science **326**, 415 (2009).

[7] S. Mostame, C. Castelnovo, R. Moessner, and S. L. Sondhi, Proc. Natl. Acad. Sci. USA **111**, 640 (2014).

[8] C. Castelnovo, R. Moessner, and S. L. Sondhi, Phys. Rev. Lett. **104**, 107201 (2010).

[9] D. Slobinsky, C. Castelnovo, R. A. Borzi, A. S. Gibbs, A. P. Mackenzie, R. Moessner, and S. A. Grigera, Phys. Rev. Lett. **105**, 267205 (2010).

[10] J. von Boehm and P. Bak, Phys. Rev. Lett. **42**, 122 (1979).

[11] P. Bak and J. von Boehm, Phys. Rev. B **21**, 5297 (1980).

[12] P. Bak, Rep. Prog. Phys. **45**, 587 (1982).

[13] P. Fischer, B. Lebech, G. Meier, B. D. Rainford, and O. Vogt, J. Phys. C: Solid State Phys. **11**, 345 (1978).

[14] R. A. Cowley, D. A. Jehan, D. F. McMorrow, and G. J. McIntyre, Phys. Rev. Lett. **66**, 1521 (1991).

[15] B. S. Shastry and B. Sutherland, Physica B+C **108**, 1069 (1981).

[16] S. Yoshii, T. Yamamoto, M. Hagiwara, A. Shigekawa, S. Michimura, F. Iga, T. Takabatake, and K. Kindo, J. Phys.: Conf. Ser. **51**, 59 (2006).

[17] S. S. Sunku, T. Kong, T. Ito, P. C. Canfield, B. S. Shastry, P. Sengupta, and C. Panagopoulos, Phys. Rev. B **93**, 174408 (2016).

[18] T. Suzuki, Y. Tomita, and N. Kawashima, Phys. Rev. B **80**, 180405(R) (2009).

[19] T. Suzuki, Y. Tomita, N. Kawashima, and P. Sengupta, Phys. Rev. B **82**, 214404 (2010).

[20] W. C. Huang, L. Huo, G. Tian, H. R. Qian, X. S. Gao, M. H. Qin, and J. M. Liu, J. Phys.: Condens. Matter **24**, 386003 (2012).

[21] K. Wierschem and P. Sengupta, Phys. Rev. Lett. **110**, 207207 (2013).

[22] Y. I. Dublenych, Phys. Rev. Lett. **109**, 167202 (2012).

[23] W. C. Huang, L. Huo, J. J. Feng, Z. B. Yan, X. T. Jia, X. S. Gao, M. H. Qin, and J. M. Liu, Europhys. Lett. **102**, 37005 (2013).

[24] J. J. Feng, L. Huo, W. C. Huang, Y. Wang, M. H. Qin, J. M. Liu, and Z. Ren, Europhys. Lett. **105**, 17009 (2014).

[25] Y. I. Dublenych, Phys. Rev. E **90**, 052123 (2014).

[26] J. Shin, Z. Schlesinger, and B. S. Shastry, Phys. Rev. B **95**, 205140 (2017).

[27] L. Regeciová and P. Farkašovský, Eur. Phys. J. B **92**, 184 (2019).

[28] P. Farkašovský and L. Regeciová, Eur. Phys. J. B **92**, 33 (2019).

[29] K. Wierschem, S. S. Sunku, T. Kong, T. Ito, P. C. Canfield, C. Panagopoulos, and P. Sengupta, Phys. Rev. B **92**, 214433 (2015).

[30] S. Michimura, A. Shigekawa, F. Iga, T. Takabatake, and K. Ohoyama, J. Phys. Soc. Jpn. **78**, 024707 (2009).

[31] K. Siemensmeyer, E. Wulf, H.-J. Mikeska, K. Flachbart, S. Gabani, S. Matas, P. Priputen, A. Efdokimova, and N. Shitsevalova, Phys. Rev. Lett. **101**, 177201 (2008).

[32] G. Misguich, T. Jolicoeur, and S. M. Girvin, Phys. Rev. Lett. **87**, 097203 (2001).

[33] T. Jolicœur, G. Misguich, and S. M. Girvin, Prog. Theor. Phys. Suppl. **145**, 76 (2002).

[34] H. Kageyama, K. Yoshimura, R. Stern, N. V. Mushnikov, K. Onizuka, M. Kato, K. Kosuge, C. P. Slichter, T. Goto, and Y. Ueda, Phys. Rev. Lett. **82**, 3168 (1999).

[35] S. Miyahara and K. Ueda, J. Phys.: Condens. Matter **15**, R327 (2003).

[36] J. Trinh, S. Mitra, C. Panagopoulos, T. Kong, P. C. Canfield, and A. P. Ramirez, Phys. Rev. Lett. **121**, 167203 (2018).

[37] J. Etourneau, J. Mercurio, A. Berrada, P. Hagenmuller, R. Georges, R. Bourezg, and J. Gianduzzo, J. Less-Common Met. **67**, 531 (1979).

[38] R. Watanuki, H. Mitamura, T. Sakakibara, G. Sato, and K. Suzuki, Physica B: Condens. Matter **378-380**, 594 (2006).

[39] S. Yoshii, T. Yamamoto, M. Hagiwara, T. Takeuchi, A. Shigekawa, S. Michimura, F. Iga, T. Takabatake, and K. Kindo, J. Magn. Magn. Mater. **310**, 1282 (2007).

[40] F. Iga, A. Shigekawa, Y. Hasegawa, S. Michimura, T. Takabatake, S. Yoshii, T. Yamamoto, M. Hagiwara, and K. Kindo, J. Magn. Magn. Mater. **310**, e443 (2007).

[41] S. Yoshii, T. Yamamoto, M. Hagiwara, S. Michimura, A. Shigekawa, F. Iga, T. Takabatake, and K. Kindo, Phys. Rev. Lett. **101**, 087202 (2008).

[42] D. Brunt, G. Balakrishnan, D. A. Mayoh, M. R. Lees, D. Gorbunov, N. Qureshi, and O. A. Petrenko, Sci. Rep. **8**, 232 (2018).

[43] See Supplemental Material at http://link.aps.org/supplemental/10.1103/PhysRevB.102.060407 for additional information and figures of the crystal growth, the out-of-plane correlation length, the dependence on the field ramp speed, the evolution with increasing temperature, magnetization curves, the variation of the propagation vectors, Bragg peaks above the freezing temperature, field cooling, the different periodicities, and of coaxial magnetic moments.

[44] D. Brunt, M. Ciomaga Hatnean, O. A. Petrenko, M. R. Lees, and G. Balakrishnan, Crystals **9**, 211 (2019).

[45] U. Staub, V. Scagnoli, Y. Bodenthin, M. García-Fernández, R. Wetter, A. M. Mulders, H. Grimmer, and M. Horisberger, J. Synchrotron Radiat. **15**, 469 (2008).

[46] U. Flechsig, F. Nolting, A. Fraile Rodríguez, J. Krempaský, C. Quitmann, T. Schmidt, S. Spielmann, and D. Zimoch, AIP Conf. Proc. **1234**, 319 (2010).

[47] S. Mata, K. Siemensmeyer, E. Wheeler, E. Wulf, R. Beyer, T. Hermannsdör, O. Ignatchik, M. Uhlarz, K. Flachbart, S. Gabán, P. Priputen, A. Efdokimova, and N. Shitsevalova, J. Phys.: Conf. Ser. **200**, 032041 (2010).

[48] H. Boysen, Phase Trans. **55**, 1 (1995).

[49] D. Brunt, G. Balakrishnan, A. R. Wildes, B. Ouladdiaf, N. Qureshi, and O. A. Petrenko, Phys. Rev. B **95**, 024410 (2017).

[50] K. Zhang and P. Charbonneau, Phys. Rev. Lett. **104**, 195703 (2010).

[51] Open data for "Evolution of field-induced metastable phases in the Shastry-Sutherland lattice magnet TmB$_4$," Zenodo, doi:10.5281/zenodo.3932115.